Article:
Nowak, A. and Hodson, A. (2014) On the biogeochemical response of a glacierized High Arctic watershed to climate change: Revealing patterns, processes and heterogeneity among micro-catchments. Hydrological Processes. Article first published online: 12 August 2014. ISSN 0885-6087

https://doi.org/10.1002/hyp.10263

On the biogeochemical response of a glacierized High Arctic watershed to climate change: Revealing patterns, processes and heterogeneity among micro-catchments

Short title: **Response of a High Arctic catchment to climate change**

Authors: Aga Nowak[1] and Andy Hodson[1,2]

[1]Department of Geography, The University of Sheffield, Winter Street, Sheffield, S10 2TN, UK

[2]Arctic Geology, University Centre on Svalbard (UNIS), Longyearbyen, Svalbard, Norway, PO Box 156, N-9171

Person for correspondence: Dr. Aga Nowak

Email: aga.nowak.09@gmail.com; Tel: +44 0114 222 7990

This article has been accepted for publication and undergone full peer review but has not been through the copyediting, typesetting, pagination and proofreading process which may lead to differences between this version and the Version of Record. Please cite this article as doi: 10.1002/hyp.10263

Abstract

Our novel study examines landscape biogeochemical evolution following deglaciation and permafrost change in Svalbard by looking at the productivity of various micro-catchments existing within one watershed. It also sheds light on how moraine, talus and soil environments contribute to solute export from the entire watershed into the downstream marine ecosystem.

We find that solute dynamics in different micro-catchments are sensitive to abiotic factors such as runoff volume, water temperature, geology, geomorphological controls upon hydrological flowpaths and landscape evolution following sea level and glacial changes. Biotic factors influence the anionic composition of runoff due to the importance of microbial SO_4^{2-} and NO_3^- production. The legacy of glaciation and its impact upon sea level changes is shown to influence local hydrochemistry, allowing Cl^- to be used as a tracer of thawing permafrost that has marine origins. We show that a "glacial signal" dominates solute export from the watershed. Therefore, although climatically driven change in the proglacial area has an influence on local ecosystems, the biogeochemical response of the entire watershed is dominated by glacially derived products of rapid chemical weathering. Consequently, only the study of micro-catchments existing within watersheds can uncover the landscape response to contemporary climate change.

Keywords: Bayelva; Svalbard; biogeochemistry; nitrification; permafrost degradation, deglaciation; microbially mediated weathering

1. Introduction

It is expected that the change in permafrost thickness that is following climate warming will have an effect on the hydrology and biogeochemistry of Arctic tundra streams (e.g. Rouse et al., 1997; Hobbie et al., 1999; Smith et al., 2005; Prowse et al., 2006; Zarnetske et al., 2007; Schuur et al., 2009). Furthermore, an increase in export of organic matter, major ions and inorganic nutrients in response to permafrost thinning is also expected to affect the

productivity of the Arctic Ocean (Tye and Heaton 2007; Frey and McClelland 2009), although the magnitude of this influence is unclear (Le Fouest et al., 2013; Tank et al., 2012). Therefore, numerous studies have been devoted to the dynamics of the permafrost table and seasonally thawing active layer (hereafter AL), which is especially susceptible to any changes in air temperatures (T_a). Although annual variations in the AL thickness strongly depend on the regional setting and seasonal weather conditions (Rachlewicz and Szczuciński, 2008), interannual variations respond to long term climatic changes that have already been observed in many parts of the Arctic (ACIA 2005; Etzelmüller et al., 2011). For example, studies from the Bayelva watershed in Svalbard (the location of the present study) have documented up to a 50% increase in AL depth over the last decade (e.g. Roth and Boike 2001; Boike 2009). This coincided with an increase in the AL thickness in other locations in Svalbard as well as in the Alaskan, Canadian and Russian Arctic (IPCC 2007), demonstrating the near-global trend in AL deepening and permafrost warming. Thus, one could expect an extensive research literature investigating the changes in physical, hydrological and biogeochemical processes in High Arctic environments that follow such AL/permafrost transformation. However, although research on soil-water interactions in Svalbard's tundra and AL have received some attention (Pecher 1994; Stutter and Billet 2003; Tye and Heaton 2007), little or no attention has been given to other important permafrost sediments, namely talus slopes and moraines (e.g. Cooper et al., 2002). This is surprising considering that most of these reactive stores of physically comminuted rock debris are commonplace in Svalbard's mountainous land surface. Therefore understanding landscape biogeochemical change here requires the integration of process studies from a range of smaller micro-catchments in glacial and proglacial environments where these sedimentary habitats are present. Such micro-catchments are most likely very chemically productive and can therefore influence the downstream evolution of glacial runoff. For example, work from Alpine or temperate glacier forefields has already shown us that the high rock-water contact and longer water residence times they afford, provide an ideal environment for microbially mediated chemical weathering reactions (e.g. Williams et al., 2006; von Rohr 2007). Additionally, young and unstable sediments in the High Arctic often lack the plants that might otherwise assimilate nutrients produced by chemical weathering. Hence, it can be expected that the sediments nearer changing glaciers might be far more capable of driving changes in solute acquisition and export from the landscape than the stable, vegetated and

up to 10^4 year old tundra surfaces that lie beyond Little Ice Age moraines. However, the prediction of changes in solute export to downstream aquatic and marine ecosystems can be challenging when we consider that studies characterizing spatial and temporal patterns in hydro-biogeochemical coupling across the High Arctic landscape are also lacking. For example, no studies in Svalbard have yet been devoted to the comparison of ion yields exported separately from tundra, talus and moraine environments. Nor have their ion yields been compared to those exported from whole catchments. This lack of important information prevents the early detection of change, because landscape signals might be masked in the first instance by dilution from the large volumes of glacial meltwater produced in the early stages of deglaciation (e.g. Nowak-Zwierz 2013; Nowak and Hodson In Press).

Hence, the two objectives of this study were firstly to examine landscape biogeochemical evolution following deglaciation and permafrost change in Svalbard, and secondly to assess how various micro-catchments contribute to solute export from the entire watershed into the downstream marine ecosystem.

Therefore, to address the first objective we focus on the spatial and temporal signal of ion production from various micro-catchments that represent young moraines, talus and soils within a High Arctic, partially glacierized watershed. Most emphasis is given to the biogeochemical processes at end of the ablation season which, we think, are especially interesting in the light of the recent findings by Nowak and Hodson (2013) in the same study site. There, it was shown that delayed water flowpaths through the AL at the end of summer are an increasingly conspicuous feature of the entire watershed's hydrograph over the last decade. To address the second objective we compare the productivity of the micro-catchments, defined as solute yields, to solute delivery by Bayelva (hereafter BAY), which drains the entire watershed into an Arctic fjord (Kongsfjorden).

2. Location

2.1 The watershed (BAY)

The study was conducted in the pro-glacial area of Bayelva watershed in Svalbard (Fig. 1). Detailed description of the whole watershed is given in Nowak and Hodson (2013; in Press), whilst the pro-glacial area is described in Westermann et al., (2010). In brief, the 32km^2 catchment is circa 50% covered by two cold-based valley glaciers: Austre and Vestre Brøggerbreen. Their meltwaters are routed through quaternary moraines onto a sandur (the floodplain formed by glaciofluvial sedimentation), where they are joined by various tributaries from neighbouring talus and soil micro-catchments to eventually be evacuated as Bayelva into Kongsfjorden. The geology of the watershed consists of red sandstones, conglomerates, quartzite, phyllites and carbonates in the southern and eastern part and further tertiary sandstone, shale, limestone and coal seams in the northern and western part (Fig. 1). Additionally, the northern part of the watershed shows evidence of being deposited in shallow marine areas (Orvin 1934; Hjelle 1993; Bruland and Hagen 2002). The catchment is located in the continuous permafrost zone with thicknesses ranging from 100 m (coastal region) to 500 m (mountainous region). During summer, its uppermost part thaws creating an AL that has been increasing significantly in recent years, and ranges from 0.5 up to 1.5m (see Roth and Boike 2001; Boike 2009; Westermann et al., 2010; Westermann et al. 2011). The annual mean (catch corrected) precipitation in the catchment during the last 35 years was just under 540 mm with the mean June-October rainfall of about 157 mm (Nowak and Hodson 2013).

2.2 The Microcatchments

Four study sites selected to represent young moraine (MM), talus (TM) and two soil micro-catchments (SM1 and SM2) were monitored during 2009 and 2010 ablation seasons (Fig. 1; Table 1).

2.1.1 Moraine micro-catchment (MM)

The MM site was created in August 2009 when the main meltwater flowpath from Austre Brøggerbreen was changed due to glacier retreat (Nowak and Hodson, In Press). In consequence, a circa 1 km river channel draining about 74% of glacial meltwaters was

abandoned (Fig. 2) and a small micro-catchment was created. It consists of Austre Brøggerbreen's ice-cored lateral moraine and the western slopes of Zeppelin mountain that includes a small sea bird breeding colony on the cliffs. The geology of MM comprised of clastic sedimentary rocks, evaporites and carbonates as well as poorly sorted rock debris such as red sandstone, quartzite, phyllite, mica and quartz-carbonate schists delivered by glacial meltwaters. No vegetation cover was recorded.

2.1.2 Talus micro-catchment (TM)

Similar to MM, TM consisted of poorly sorted rock debris that included carbonate rocks, evaporates and clastic sedimentary rocks. However, small patches of vegetation including mosses, *Dryas*, *Salix* and *Carex* communities were recorded in the vicinity of the stream (Fig. 3). Additionally, the southern part of the micro-catchment was occupied by a rock glacier and northern part was covered by patterned ground that indicated frost heaving in the area.

2.1.3 Soil micro-catchments (SM1, SM2)

The two soil micro-catchments SM1 and SM2 were selected on the basis of differences in geology, vegetation cover and the type of the river bed. The geology of the former consisted of chert, siliceous shale, sandstone, limestone, sedimentary rocks and coal seams. The micro-catchment was fully covered by a mixture of vegetation that included *Dryas*, *Salix* and *Carex* communities as well as variety of mosses also growing on the partially sandy bed of the stream. The geology of the SM2 additionally consisted of carbonate rocks and evaporates located at Schetelig mountain slopes. In contrast to SM1, SM2 was only partially covered by vegetation and had a rocky stream bed that was dominated by algae (Fig. 4).

3. Methods

3.1 Meteorological conditions

Meteorological data for Ny-Ålesund area has been downloaded from eklima.met.no (2013) for weather station (no. 99910) located at 78.923N, 11.933E at 8 m a.s.l. Precipitation types were deduced from T_a and classified as snow (when $T_a<0^oC$) or rain (when $T_a>0^oC$). Measured precipitation data were then corrected for catch by the value of 1.15 (rain) and

1.65 (snow) after Killingtveit (2004). Elevation gradient correction of 19% per 100m was used to further correct the data for elevation change. Detailed description of the Bayelva catchment hydrology and meteorological conditions between 1974-2010 is presented in Nowak and Hodson (2013).

3.2 Hydrological monitoring

Campbell Scientific CR800 and CR1000 data loggers were used to monitor water stage, electrical conductivity and water temperature at sampling sites during both ablation seasons (see Table 2 and Figure 1 for details). Data were collected every 30 sec, averaged and then recorded every 15 min. The salt dilution method (Moore 2005) was performed after sampling at all four sites to estimate discharge rating curves. They were then used along with water stage to calculate hourly discharge at every micro-catchment with errors of ca. 10% (Hodson 1994). In order to collect representative water samples from the moraine, talus and tundra environments, each hydrological monitoring station and water sampling point was located at the micro-catchment boundary, where water was draining the entire area of interest (see Figure 1 and Table 1).

3.3 Water sampling

In 2009 sampling was undertaken from the beginning of the ablation season when the streams were opening in the melting snowpack, until the cessation of flow. In 2010 the sampling commenced one week after the beginning of snowpack runoff and when most of the snowpack had melted at both SM sites. Water samples were collected with a pre-rinsed 250 mL polyethylene bottle and filtered within 12 hrs through a 0.45 µm Whatman cellulose nitrate filter papers using a Nalgene filtration unit. After filtration, samples were stored without air at +4^{o}C in 60 mL sterile, polypropylene bottles for no longer than 3 months. No contamination was detected in deionized water blanks collected and examined along with other streamwater samples. A comparison of hydrological monitoring and water sampling at every site during the 2009 and 2010 field campaigns is presented in Table 2.

3.4 Laboratory analyses

Sample pH was measured directly after collection with a daily calibrated handheld pH meter. The precision of the meter was ± 0.01 pH unit and the electrode efficiency was

always above 95%. Concentrations of major ions such as Ca^{2+}, Mg^{2+}, Na^{+}, K^{+}, Cl^{-}, SO_4^{2-} and nutrients such as NH_4^{+}, NO_3^{-}, PO_4^{3-} were determined by ion chromatography with the use of a Dionex IC90. The detection limit of all analyses was 0.001 mg L^{-1} and the precision errors were below 5%. Dissolved Si was determined by wet chemistry using a Skalar automatic nutrient analyser employing the molybdenum blue method. The precision errors of all Si analyses were also below 5%. Total alkalinity (HCO_3^{-}) was calculated from ion charge balance after Wolf-Gladrow et al., (2007) when all the ions were analysed.

3.5 Solute provenance and yields

Ion concentrations were separated into marine and crustally derived components (hereafter ssX and *X, where X is the solute of interest) after assuming that Cl^{-} was of marine (sea salt) origin. Therefore, ssX were calculated after Holland (1978) from standard marine ratios of ions to Cl^{-} in seawater. Then, *X were calculated by the subtraction of ssX from their total concentration. Lastly, the sum of rock and microbially produced SO_4^{2-} (hereafter $*SO_4^{2-}$) was calculated after subtraction of the sum of $ssSO_4^{2-}$ and atmospheric SO_4^{2-} from the total SO_4^{2-} concentrations. The sum of $ssSO_4^{2-}$ and atmospheric SO_4^{2-} was calculated using the average snowpack SO_4^{2-}/Cl^{-} ratio from snow samples collected at each micro-catchment (data not shown).

Ion yields were calculated according to Hodson et al., (2005) by summing the product of daily total stream discharge and ion concentration pairs, before dividing by the individual micro-catchment area. Since in some cases sampling was not undertaken every day, missing daily concentrations were estimated by either linear interpolation (when samples were collected every second day) or by best fit regression models of ion concentration and the stream discharge (when samples were collected every third and fourth day).

3.6 Stable isotope analyses

To compare microbially-mediated dynamics of nitrate among the micro-catchments, samples from 2010 were also analysed for $\delta^{15}N$ and $\delta^{18}O$ in NO_3^{-} at the School of Environmental Sciences, University of East Anglia using the bacterial denitrifier method following Kaiser et al., (2007). This allows determination of $\delta^{15}N$ and $\delta^{18}O$ with a precision of

0.2‰ for $\delta^{15}N$ and 0.5‰ for $\delta^{18}O$ in samples containing more than 10 nmol L^{-1} of NO_3^-. Full details are reported by Ansari et al., (2013), who discuss a set of samples from local snowpack and glaciers that were collected and analysed at the same time as the present study.

4. Results

4.1 Meteorological conditions

The ablation season in 2009 was colder and wetter than 2010. Therefore, mean T_a during summer of 2009 were lower by between 1 and 1.5^oC in May, June and October (when runoff was still occurring). Rainfall was the most dominant form of summer precipitation during both years however, nearly three times more rainfall was recorded during 2009. Additionally, in 2010, rainfall was mostly confined to October, which received nearly 50% of the total wet precipitation recorded during summer. Snowfall was recorded only in May and October during both ablation seasons. In May it accounted for 17% (2009) and 0.2% (2010) of the total precipitation, while in October for 66% (2009) and 16% (2010).

4.2 Solute concentrations

The time series of key solutes recorded during the two observation periods at each micro-catchment are presented in Fig. 5. A full description of the same solutes recorded at BAY between 1991 and 2010 is given in Nowak-Zwierz 2013, and is used here for comparative purposes (years 2009 and 2010).

Moraine micro-catchment

A sudden increase in concentrations of solutes commonly associated with carbonate weathering (namely $*Ca^{2+}+*Mg^{2+}$ and HCO_3^-) was recorded around Day 217 (2009) and Day 207 (2010), which occurred when water discharge decreased markedly (see Fig. 5a). Interestingly, after those days, acquisition of $*Ca^{2+}+*Mg^{2+}$ did not follow the pattern in HCO_3^- acquisition. Instead, changes in $*Ca^{2+}+*Mg^{2+}$ were accompanied by an increase in solutes associated with silicate weathering (namely Si, and $*Na^{+}+*K^{+}$; see Fig. 5b) as well as $*SO_4^{2-}$ (Fig. 5c). The concentrations of $*Na^{+}+*K^{+}$ and NO_3^- reached the highest levels

recorded amongst all of the micro-catchments. NH_4^+ was recorded few times during July 2010 and ranged from 3 to 19 µg L^{-1}. No PO_4^{3-} was detected. Lastly, pH of the stream varied during both ablation seasons between 7.5 and 8.0 (Fig. 6).

Talus micro-catchment

Although the concentrations of ions recorded at TM were different to those recorded at MM, the behaviour of solute acquisition was similar. The same sudden increase in ion concentrations on Day 217 (2009) and 207 (2010) was also observed. The exceptions were HCO_3^- and $*Na^+ + *K^+$, whose concentrations increases were much less pronounced and even declined in the case of HCO_3^-. Additionally, concentrations of $*Ca^{2+} + *Mg^{2+}$ and $*SO_4^{2-}$ were amongst the highest recorded at all micro-catchments. NH_4^+ was only recorded a few times during July 2010 and ranged from 3 to 25 µg L^{-1}. Similarly to MM, no PO_4^{3-} was detected. pH varied between 7.3 and 8.2.

Soil micro-catchments

In contrast to MM and TM, concentrations of all ions recorded at SM1 and SM2 sites were characterized by a steady increase during the ablation season without any sudden changes as described above (the exception was Si in 2009 which will be discussed below). No PO_4^{3-} was detected at either sites and pH values (were similar and varied between 6.1 and 8.3 (SM1) and 7.7 – 8.1 (SM2). Low pH values (< 7.7) at SM1, representing snowmelt, were recorded at the end of June 2009. Despite the similarities in temporal pattern of solute acquisition, differences in the solute concentrations were observed between the two soil micro-catchments. Therefore, concentrations of ions at SM1 were markedly higher than at SM2. For example, the concentrations of Si in 2010 were the highest observed in all of the micro-catchments. Also, a marked increase in Cl^- concentrations distinguished SM1 from all other micro-catchments. Such a marked and steady increase in Cl^- was a surprise to us and will be explored in detail later in the paper. Additionally, no NH_4^+ was recorded at SM1 while at SM2, similarly to TM and MM, NH_4^+ was recorded a few times during July 2010 and varied between 3 and 19 µg L^{-1}.

4.3 Solute yields

A comparison of solute yields from all micro-catchments and from the entire watershed (BAY) is presented in Table 3. Data for BAY was taken from Nowak and Hodson (In Press) and are used here as a basis for establishing the efficacy of solute export from the micro-catchments. The general characteristics in ion yields at all sites were similar. Therefore, HCO_3^-,*Ca^{2+} and SO_4^{2-} showed the largest yields and Si and NO_3^- the lowest (NH_4^+ is not presented). However, the magnitude of ion yields varied among the sites for reasons that are explored in the discussion. Variations between the years were also apparent, for example due to differences in snowmelt capture during our monitoring (for SM1) and the length of monitoring period (for MM).

4.4 Stable isotopes

Variations in stable isotopes (expressed here as $\delta^{15}N$ and $\delta^{18}O$ values relative to atmospheric-N_2 and Vienna Standard Mean Ocean Water respectively) are presented in Fig. 7 and 8. A decreasing trend in $\delta^{18}O$ was observed at SM1 which was neither observed at TM nor accompanied by any trend in $\delta^{15}N$ (at either site, see Fig. 7). Fig. 8 shows that the $\delta^{18}O$ values at this site were far lower than those observed in snowpack of this region, and in the BAY during early summer (the only available data being from before Day 186, when snowmelt caused high concentrations in the glacial outflow). The values at SM1 were also marginally lower than those from the other micro-catchments, although data was sparse at SM2 and MM. Interestingly, the $\delta^{18}O$ values from SM1 lay below the predicted range for microbial NO_3^- (Fig. 8) and estimated under the assumption that one atom of atmospheric O_2 ($\delta\ ^{18}O$ = 23.5 ‰) and two atoms of water oxygen (range used here: -15 to -6.8 ‰) are assumed to oxidise the N substrate during nitrification (Casciotti et al., 2002). For $\delta^{15}N$, the data was between -0.6 and + 6.0 ‰ at all sites except the BAY, where the range was greater (-6.0 to 3.2 ‰). Therefore the $\delta^{15}N$ values in the micro-catchments compare favourably to the range of $\delta^{15}N$ for soil organic matter and ammonium recorded by previous research in the area and used to define the range of microbial NO_3^- in Fig. 8.

5. Discussion

5.1 Landscape biogeochemical evolution following deglaciation and permafrost change in Svalbard

In this section we focus on comparing solute acquisition and their transfer dynamics in the different micro-catchments using chemical weathering reactions that are already widely described in the literature (e.g. Tranter et al. 1993; Tranter et al. 1996; Anderson et al. 1997; Hodgkins et al. 1998; Brown 2002; Hodson et al. 2005). To establish the broad categories of chemical weathering processes we employ the statistical approach described by Nowak and Hodson (In Press), Nowak-Zwierz 2013, and Wadham et al., (2010). In so doing, a set of regression models between the solutes was produced and presented in Table 4. Scatterplots in Fig. 9 show the data used to define those models as well as the corresponding associations for main glacial meltwater channel (BAY).

5.1.1 Temporal and spatial changes in solute acquisition

Moraine micro-catchment

Two groups: *early* (pre-snowmelt, before days 217 in 2009 and 211 in 2010) and *late season* (post-snowmelt, after the above days) were distinguishable in the MM dataset (Fig. 5). Meltwater chemistry during the *early season* was dominated by carbonate carbonation (similarly to BAY). However, regression models presented in Table 4 indicated that other processes of ion acquisition were also operating in the environment. Those were most likely dissolution of gypsum/anhydrite as well as dissolution of carbonate and silicate minerals coupled to sulphide oxidation. Moreover, it is probable that weathering of dust supplied from the melting snowpack contributed to the initial ion concentration (see Tranter et al. 1996).

As the season progressed a marked change in solute acquisition was observed. Carbonate carbonation was no longer a major process supplying the ions. Instead, dissolution of gypsum was much more pronounced and accompanied by silicate dissolution coupled to sulphide oxidation (see also Fig 5a,b). A further interesting artefact of the silicate mineral weathering was revealed by *Model 8* (Table 4), where increase in slope during the *late season* indicated additional source of $*K^+$. We interpret this as a sign of K-feldspar

weathering in the ice cored moraines which became an increasingly important source of base flow, due largely to the development of their active layer and the demise of the snow pack. A distinct feature of the moraines was the presence of fine, comminuted red sandstones transported down glacier from the southern part of the watershed. This feature was not present in any of the other micro-catchments and thus most likely explains why the concentrations of $*K^+$ were greatest here. Lastly, (unlike in BAY) *Models 6* and *7* (Table 4) suggested that NO_3^- production was concomitant with sulphide oxidation and silicate weathering. A case is therefore made for nitrification in the discussion below, when the isotope data are examined.

Talus micro-catchment

Samples collected at TM were also divided into *early* and *late season* groups following the same justification as for MM. However, in contrast to MM and BAY, during the *early season*, carbonate carbonation was much less pronounced and the higher proportion of ions was also supplied by gypsum/anhydrite dissolution accompanied by a weak signal from silicate weathering. Interestingly, Fig. 5a,c clearly shows a distinct switch in chemical weathering between *early* and *late seasons* when ions were no longer acquired by carbonate carbonation at all, and the major reaction was gypsum/anhydrite dissolution. Considering the similarity in geological settings of both TM and MM, such a change in ion acquisition between those sites may be the result of different geomorphological characteristics (i.e. the presence of rock glacier and patterned ground at TM) and/or landscape maturity. Furthermore, *Model 7* and Fig. 9 indicated more pronounced nitrification than at MM, also resulting in greater nitrate flux (2009).

Soil micro-catchments

In contrast to both MM and TM, no marked change in solute concentrations were recorded on Days 217 (2009) and 211 (2010) at SM1 and SM2. Instead a steady increase of ions was captured from almost the beginning until the end of ablation seasons. In 2010, this was a consequence of post-snowmelt sampling and therefore, the results demonstrate only the chemistry typical of *late season*. However, sampling at SM1 in 2009 was undertaken throughout the whole ablation season, so the lack of the sudden transition in solute acquisition observed at TM and MM requires further explanation. We believe this was most

likely related to the influences of runoff regime, geomorphology and biological activity. For example, in contrast to other sites, the SM1 stream collects water only very slowly from the surrounding low relief hill slopes. Consequently, water slowly draining through tundra soils caused increased the residence time and therefore enhanced solute acquisition for much of the observation period. Field observations showed that SM1 had the highest soil moisture (data not shown) of all the micro-catchments, with many fully saturated, expansive areas near the channel that maintained water saturation well into August (Fig. 4).

A decline in Si concentrations around Day 200 in 2009 coincided with a significant drop in concentrations of NO_3^-, a fall in water discharge (to $6x10^{-4}$ m^3 sec^{-1}) and an increase in water temperature to above 7^oC (data not shown). We believe this was linked to a diatom bloom at SM1 that was not observed at all the other micro-catchments where faster-flowing drainage and lower water temperatures were unlikely to support such a phenomenon. After recovery from uptake by diatoms, temporal changes in Si acquisition recorded at SM1 mimicked those at TM and MM and thus reflected the transition from the *early to late season.*

The processes of ion acquisition also differed between SM1 and SM2 (Table 4, Fig. 5 and 9). At SM1, the main reaction supplying ions was calcite carbonation, whilst carbonation of dolomite also occurred at SM2, reflecting the geological heterogeneity of the watershed. Furthermore, the difference was also noticeable in the intensity of sulphide oxidation that was accompanied by almost stoichiometric silicate weathering (uncharacteristic for glacial meltwaters, e.g. at BAY; see Hodson et al., 2002). Both sulphide oxidation and silicate weathering were more pronounced at SM2 according to the slope values of regression *Model 9* (Table 4), in spite of lower concentrations than at SM1.

Lastly, a marked *late season* increase in Cl^- concentrations during both ablation seasons was unique to SM1. This cannot be attributed to the elution of snow because the snowpack retreated from this part of the catchment first and there were no persistent snowbanks. Marine aerosol inputs of Cl^- caused by high winds and evaporation effects were not responsible for such increase because these processes should have influenced streams across the entire proglacial area. Nor could the Cl^- inputs be attributed to rock weathering, as the geological conditions are not favourable and simple laboratory dissolution reactions

using 10 g L^{-1} suspensions of freshly milled rock in deionised water showed no significant increase in Cl^- concentrations with time (Hodson, Unpublished Data). It should be noted however, that SM1 is the only micro-catchment that lies entirely within the former marine limits. For example, marine bivalve shells are abundant in the active layer (field observation; see also Fig. 10), and so we attribute the Cl^- increase to the release of marine salts from the permafrost of this former sea bed. The mobility of Cl^- is such that it may be rapidly leached into the stream as the active layer deepens, making its seasonal concentration increase a potentially sensitive indicator of marine permafrost degradation in low elevation catchments such as SM1.

5.1.2 The fingerprint of microbial activity in the micro-catchments

The use of correlations between Si, NO_3^- and $*SO_4^{2-}$ to detect microbial activity in the micro-catchments (Table 4) was further supported by the $\delta^{15}N$ and $\delta^{18}O$ values for NO_3^- due to their proximity to the predicted range of microbial nitrate (Fig. 7 and 8). However, at TM, the $\delta^{18}O$ values were higher than the microbial NO_3^- range, implying a little more snowpack-derived NO_3^- was present (in agreement with the observed persistence of snow cover in the TM watershed). Further, low $\delta^{18}O$ values in SM1 NO_3^- show that nitrification was effective throughout the entire summer. This was surprising, because it was expected that assimilation of NO_3^- by vegetation would suppress the nitrification signal in runoff until senescence occurred (Tye et al., 2008). In addition, the $\delta^{18}O$ values in SM1 NO_3^- were in fact lower than the predicted range of microbial NO_3^-, as was observed by Tye et al., (2008) just outside the Bayelva watershed. In Casciotti et al's (2010) experimental study of oxygen isotope systematics during NH_4^+ oxidation, both fractionation and isotope exchange effects are plausible explanations for such low values. The most robust interpretation of the present study is therefore that nitrification dominates the production of the NO_3^- that is flushed from the SM1 micro-catchment by runoff very soon after the removal of the snowpack. The data from SM2 and MM, although sparse, also suggest that nitrification is important in these other micro-catchments, whilst the marginally higher values for the TM suggest that a small proportion of atmospheric NO_3^- also enters the system from the high elevation snow that is present here.

5.2 Contribution of the micro-catchments to solute export from the entire watershed

The important differences in solute dynamics in the landscape units represented by the various micro-catchments are easily noticeable (e.g. in Fig. 5 and 9, Table 4), yet they are almost impossible to establish from measurements conducted at BAY (Nowak and Hodson 2013) and have not yet been detected in other watershed scale studies in Svalbard. For example, the average concentrations of ions recorded at BAY were up to two (HCO_3^-, $*Ca^{2+}$ + $*Mg^{2+}$), four (Si), seven (NO_{3-}) and ten times ($*SO_4^{2-}$) lower than those recorded at the micro-catchments (Fig. 9), because the water flux through Bayelva was almost two orders of magnitude greater and therefore significantly diluted by icemelt.

Water flux has a first order control over solute yields (Anderson et al., 1997) as is evident in their inter-annual variability (Table 3). The area-weighted solute yields of the micro-catchments were therefore used to see how they influence the solute flux from the entire watershed. In so doing, the different micro-catchments were assumed to be representative of the total moraine (area 3.06 km^2), talus (6.72 km^2) and tundra soils (4.18 km^2, 22% of which was similar to SM1 and 78% to SM2) in the deglacierized area (areas according to www.svalbardkartet.npolar.no, 2013). The solute yields for 2010 (Table 3) were then multiplied by the representative areas to estimate the solute fluxes from each landscape unit. Fig. 11 shows the combined solute fluxes expressed as a proportion of the total watershed solute flux at BAY. As expected, the up-scaled solute fluxes from the aggregated micro-catchments never accounted for 100% of the solute flux due to missing terms in the balance calculations, namely large solute flux associated with the glacial inputs (not monitored in this study; see Nowak-Zwierz 2013) and error (ca. 15 – 25% for each flux estimates following Hodson et al., 2005). For example, the sum of micro-catchments accounted for just 17% of the Cl^- flux during 2010, indicating a significant input from snowmelt. Hodson et al., 2005 have shown that the Cl^- budget for the watershed is easily "closed" by accounting for snowmelt in this case using the 1999 and 2000 dataset and applying it to the entire watershed (BAY). We confirmed that the glacial input could easily account for the difference in other hydrological years after estimating the product of summer melting (using glacier mass balance data) and average Cl^- concentrations reported

in supraglacial streams at this site (1.23 mg L^{-1} Hodson et al., 2002). However, the same closure in the solute budgets could not be achieved with the other ions, especially with respect to those derived from carbonate and silicate weathering. Nor could error analysis account for the different solute budget calculations for these ions, since they would require changes in the mean composition of micro-catchment streams that were unacceptable when compared to the range of values reported by earlier work (Hodson, 1994 and Hodson et al., 2002). The "missing" HCO_3^-, Ca^{2+}, Mg^{2+}, K^+ and Si were therefore acquired by glacial meltwaters from paraglacial fine sediment weathering (c.f. Fairchild et al., 1999) and shallow groundwater exchange, most likely in the hyporheic zone of the floodplain. This is also supported by the resent work presented in Nowak and Hodson (In Press) where it is shown that even a watershed accommodating cold-based glaciers and underlain by continuous permafrost has significant chemical weathering potential due to the presence of fresh fine reactive sediments released by the retreat of the glacier and rock-water contact at a range of time scales. Furthermore, the study also indicates the importance of the hyporheic zone in generation of solutes. This was also explored in front of Antarctic cold-based glaciers of the McMurdo Dry Valleys where only glacial inputs of water to the glacier forefield are present (see Gooseff et al., 2013). Further research involving direct instrumentation and sampling of the proglacial sandur environment is therefore essential in order to better understand landscape solute fluxes during deglaciation.

The comparison of the solute flux from the entire watershed and the micro-catchments resulted in an unexpected discovery. Unlike crustally derived solutes described above, the aggregated micro-catchment flux estimates for NO_3^- and $*SO_4^{2-}$ represented more than 80% and 60% of the observed riverine flux at BAY, most of which was derived from moraine and talus environments. This shows the importance of microbial processes in these low water flux components of the deglacierized part of the watershed. It also reveals watershed potential for fertilization of down-stream marine environments with nutrients such as NO_3^-, $*SO_4^{2-}$, Si (Nowak-Zwierz 2013) and P that can also be associated with Fe^{3+} (Hodson et al., 2004). Furthermore, a recent study in an Alaskan temperate fjord system by Fellman et al., (2010) showed that glacially derived dissolved organic carbon can enhance marine bacterial production. Yet, at present, most Svalbard studies that examine the response of primary and secondary producers in the marine environment to climate change only give emphasis

to spring season algal blooms associated with sea ice melt (e.g. Hop at al., 2002; Hodal et al., 2012). Therefore here we show that summer input of nutrients into marine environments now needs to be considered so that biological production can be better understood after the spring bloom.

Lastly, our study also demonstrates for the first time that elevated concentrations of Cl^- can be used as a signal to record the biogeochemical consequences of melting permafrost of marine origin. This signal indicates that the legacy of glaciation is still strongly apparent through the impact upon sea level change and the slow, gradual release of marine solutes from parts of the landscape uplifted since the end of the last glacial maximum.

6. Conclusions

Our novel study of moraine, talus and soil micro-catchments within High Arctic watershed helps to understand landscape biogeochemical evolution following deglaciation and permafrost change. It also sheds light on how those environments contribute to solute export from the entire watershed and into the downstream marine ecosystem.

We show that seasonality in chemical weathering is strongest at sites where drainage is rapid and not restricted. Solute dynamics in different micro-catchments are also sensitive to other abiotic factors such as runoff volume, water temperature, geology, geomorphological controls upon hydrological flowpaths and landscape evolution following sea level and glacial changes.

Biotic factors also influence the anionic composition of micro-catchment runoff via microbial SO_4^{2-} and NO_3^- production that is responsible for as much as 60 and 80 % (respectively) of the total $*SO_4^{2-}$ and NO_3^- fluxes from the entire watershed.

Young environments nearest to the retreating glacier are characterized by high yields of solutes such as $*Ca^{2+}$, HCO_3^-, $*Mg^{2+}$ and $*SO_4^{2-}$ due to the presence of fine reactive sediments. Those also provide an environment for microbially mediated chemical weathering reactions and the production of nutrients such as NO_3^-. Interestingly, nitrification is occurring with similar intensity at all micro-catchments, regardless landscape

maturity. However, in younger environments, nutrients fluxes are larger and therefore can have a bigger effect on the downstream marine ecosystem.

We also find that changes in permafrost have the most noticeable effect in the marine sediments uplifted since the last glacial maximum, which are now subjected to erosion, chemical weathering and ground thaw and influence the levels of marine derived ions such as Cl^-.

Lastly, the comparison between the micro-catchments and solute fluxes exported from the entire watershed into High Arctic fjord indicates that, despite large $*SO_4^{2-}$ and NO_3^- yields from the aforementioned micro-catchments, a "glacial signal" dominates solute export from the watershed via a combination of quick weathering reactions of fine reactive sediments at the glacier terminus, rapid in-stream weathering of suspended sediments and processes occurring in the hyphoreic zones of the floodplain.

Therefore, although climatically driven change in the proglacial area such as deepening of the active layer and thawing of the permafrost has an influence on local ecosystems, the biogeochemical signal from the entire watershed (solute fluxes entering marine environment) is dominated by glacially derived products of rapid chemical weathering. Consequently only a study of micro-catchments existing within the watershed can uncover the landscape response to contemporary climate change.

Acknowledgments

This research was funded by a Marie Curie Initial Stage Training Network (NSINK- Sources, sinks and impacts of atmospheric nitrogen deposition in the Arctic, project number R/123386). The authors would like to thank DNMI for the provision of meteorological data as well as Dr. Jan Kaiser and Dr. Alina Marca from School of Environmental Sciences at the University of East Anglia for determination of NO_3^- isotopes. We also thank Phil Blaen and Dr. Tristram Irvine-Fynn for excellent field assistance during 2009 and 2010 field seasons. Furthermore, the authors would like to thank NERC for providing accommodation and support during the fieldwork in Ny-Ålesund.

References

ACIA. 2005. Arctic Climate Impact Assessment. Cambridge University Press.

Anderson SP, Drever JI, Humphrey NF. 1997. Chemical weathering in glacial environments. *Geology* **25 (5);** 399-402.

Ansari AH, Hodson AJ, Heaton THE, Kaiser J and Marca-Bell A. 2013. Stable isotopic evidence for nitrification and denitrification in a High Arctic glacial ecosystem. *Biogeochemistry* **113**; 341-357. DOI:10.1007/s10533-012-9761-9.

Boike J. 2009. SPARC and disappearing permafrost – a story from Bayelva in Svalbard. Svalbard 25 Science Forum. http://ssf.npolar.no/pages/news318.htm.

Brown GH. 2002. Glacial meltwater hydrochemistry. *Applied Geochemistry* **17;** 855-883.

Bruland O and Hagen JO. 2002. Mass Balance of Austre Brøggerbreen (Spitsbergen), 1971-1999, modelled with the precipitation-run-off model. *Polar Research* **21**: 109-121.

Budantseva NA, Vasilchuk AK, Zemskova AM, Chizhova YuN, Vasilchuk YuK, Christiansen HH. 2012. Delta ^{18}O variations in late Holocene ice-wedges and winter air temperature variability in the Yamal Peninsula, Russia and in Adventdalen, Svalbard. *International Conference on Permafrost (ICOP) Proceedings* **10**, 2: 41-45.

Casciotti KL, Sigman DM, Galanter Hastings M, Bohlke JK and Hilkert A. 2002. Measurement of the oxygen isotopic composition of nitrate in marine and fresh waters using the denitrifier method. *Anal chem* **74**: 4905–4912.

Cooper R J, Wadham JL, Tranter M, Hodgkins R, Peters NE. 2002. Groundwater hydrochemistry in the active layer of the proglacial zone, Finsterwalderbreen, Svalbard. *Journal of Hydrology* **269**: 208–223.

Etzelmüller B, Schuler T, Isaksen K, Christiansen H, Farbrot H, Benestad R. 2011. Modelling the temperature evolution of Svalbard permafrost during the 20th and 21st century. *The Cryosphere* **5**: 67-79.

Fellman J, Spencer RGM, Edwards R, D'Amore D, Hernes PJ, Hood E. 2010. The impact of glacier runoff on the biodegradability and biochemical composition of terrigenous dissolved organic matter in near-shore marine ecosystems. *Marine Chemistry,* DOI:10.1016/j.marchem.2010.03.009.

Frey K and McClelland J. 2009. Impacts of permafrost degradation on Arctic river biogeochemistry. *Hydrological Processes* **23**: 169-182.

Gooseff MN, Barrett JE, Levy JS. 2013. Shallow groundwater systems in a polar desert, McMurdo Dry Valleys, Antarctica. *Hydrogeology Journal* **21 (1)**: 171-183.

Hjelle A. 1993. The geology of Svalbard. *Norskpolar Institutt Handbok* **7**.

Hobbie JE, Peterson BJ, Bettez N, Deegan L, O'Brien WJ, Kling GW, Kipphut GW, Bowden WB, Hershey AE. 1999. Impact of global change on the biogeochemistry and ecology of an Arctic freshwater system. *Polar Research* **18 (2)**; 207-214.

Hodal H, Falk-Petersen S, Hop H, Kristiansen S, Reigstad M. 2012. Spring bloom dynamics in Kongsfjorden, Svalbard; nutrients, phytoplankton, protozoans and primary production. *Polar Biology* **35**; 191-203.

Hodgkins R, Tranter M and Dowdeswell JA. 1998. The hydrochemistry of runoff from a 'cold-based' glacier in the High Artic (Scott Turnerbreen, Svalbard). *Hydrological Processes* **12 (1)**; 87-103.

Hodson AJ. 1994. Climate, hydrology and sediment transfer process interactions in a sub-polar glacier basin. PhD Thesis, University of Southampton, Southampton, UK.

Hodson A, Tranter M, Gurnell A, Clark M and Hagen JO. 2002. The hydrochemistry of Bayelva, a high Arctic proglacial stream in Svalbard. *Journal of Hydrology* **257**: 91–114.

Hodson A, Mumford P, Lister D. 2004. Suspended sediment and phosphorus in proglacial rivers: bioavailability and potential impacts upon the P status of ice-marginal receiving waters. *Hydrological Processes* **18(32)**: 2409-2422.

Hodson AJ, Mumford PN, Kohler J and Wynn PM. 2005. The High Arctic glacial ecosystem: new insights from nutrient budgets. *Biogeochemistry* **72**: 233-256.

Holland HD. 1978. The Chemistry of the Atmosphere and Oceans. *Wiley*: New York.

Hop H, Pearson T, Hegseth EN, Kovacs KM, Wiencke C, Kwasniewski S, Eiane K, Mehlum F, Gulliksen B, Wlodarska-Kowalczuk M, Lydersen C, Weslawski JM, Cochrane S, Gabrielsen GW, Leakey RJG, Lønne OJ, Zajaczkowski M et al. 2002. The marine ecosystem of Kongsfjorden, Svalbard. *Polar Research* **21(1):** 167-208.

IPCC 2007. The Physical Science Basis. Contribution of Working Group I to the Fourth Assessment Report of the Intergovernmental Panel on Climate Change. Cambridge, United Kingdom and New York, NY, USA, Cambridge University Press.

Kaiser J, Hastings MG, Houlton BZ et al. 2007. Triple oxygen isotope analysis of nitrate using the denitrifier method and thermal decomposition of N_2O. *Analytical Chemistry* **79**: 599–607.

Killingtveit A. 2004. Water balance studies in two catchments on Spitsbergen. Northern Research Basins Water Balance Proceedings of a workshop held at Victoria, Canada, March 2004. IAHS Publishing 290.

Le Fouest V., Babin M., Tremblay J. E. 2013. The fate of riverine nutrients on Arctic shelves. Biogeosciences, 10:3661-3677.

Moore RD. 2005. Slug injection using salt in solution. *Watershed Management Bulletin* **8 (2)**. 1-6.

Nowak A and Hodson A. 2013. Hydrological response of a High Arctic catchment to changing climate over the past 35 years; A case study of Bayelva River watershed, Svalbard. *Polar Research* **32**; 19691. http://dx.doi.org/10.3402/polar.v32i0.19691.

Nowak-Zwierz A. 2013. Hydrological and biogeochemical response of a High Arctic glacierized catchment to climate change; A long term study from Bayelva watershed; Svalbard. PhD Thesis, University of Sheffield, Sheffield, UK.

Orvin AK. 1934. *Geology of the Kings Bay region, Spitsbergen*. Skrifter om Svalbard og Ishavet 57.

Pecher K. 1994. Hydrochemical analysis of spatial and temporal variations of solute composition in surface and subsurface waters of a high arctic catchment. *Catena* **21:** 305-327.

Prowse TD, Wrona FJ, Reist JD, Gibson JJ, Hobbie JE, Lévesque LMJ, Vincent WF. 2006. Climate Change effects on hydroecology of Arctic freshwater ecosystems. *Journal of the Human Environment* **35 (7)**: 347-358.

Rachlewicz G and Szczuciński W. 2008. Changes in thermal structure of permafrost active layer in a dry polar climate, Petuniabukta, Svalbard. *Polish Polar Research* **29 (3)**: 261–27.

von Rohr MR. 2007. The role of microbially mediated weathering on glacier f

in October 2013.

Roth K and Boike J. 2001. Quantifying the thermal dynamics of a permafrost site near Ny-Ålesund, Svalbard. *Water Resources Research* **37**; 2901-2914.

Rouse WR, Douglas MSV, Hecky RE, Hershey AE, Kling AE, Lesack L, Marsh P, McDonald M, Nicholson BJ, Roulet NT, Smol JP. 1997. Effects of climate change on the freshwaters of Arctic and Subarctic North America. *Hydrological Processes* **11**: 873-902.

Schuur EAG, Vogel JG, Crummer KG, Lee H, Sickman JO, Osterkamp TE. 2009. The effect of permafrost thaw on old carbon release and net carbon exchange from tundra. *Nature* **459**. DOI: 10.1038/nature08031.

Smith LC, Sheng Y, MacDonald GM, Hinzman LD. 2005. Disappearing arctic lakes. *Science* **308**: 1429.

Stutter M and Billett M. 2003. Biogeochemical controls on streamwater and soil solution chemistry in a High Arctic environment. *Geoderma* **113:** 127-146.

Tank SE., Manizza M., Holmes RM., McClelland JW., Peterson BJ. 2012. The Processing and Impact of Dissolved Riverine Nitrogen in the Arctic Ocean. Estuaries and Coasts 35:401-415.

Tranter M, Brown GH, Raiswell R, Sharp MJ, Gurnell AM. 1993. A conceptual model of solute acquisition by Alpine glacial meltwaters. *Journal of Glaciology* **39**; 573-581.

Tranter M, Brown GH, Hodson AJ and Gurnell AM. 1996. Hydrochemistry as an indicator of subglacial drainage system structure: A comparison of Alpine and sub-polar environments. *Hydrological Processes* **10 (4)**; 541-556.

Tye A and Heaton T. 2007. Chemical and isotopic characteristics of weathering and nitrogen release in non-glacial drainage waters on Arctic tundra. *Ceochimica et Cosmochimica Acta* **71**: 4188-4205.

Wadham JL, Tranter M, Skidmore M, Hodson AJ, Priscu J, Lyons WB. 2010. Biogeochemical weathering under ice: Size matters. *Global biogeochemical Cycles* **24**; GB3025, DOI: 10.1029/2009GB003688.

Westermann S, Wollschläger U, Boike J. 2010. Monitoring of active layer dynamics at a permafrost site on Svalbard using multi-channel ground-penetrating radar. *The Cryosphere* **4**: 475-487.

Westermann S, Langer M, Boike J. 2011. Spatial and temporal variations of summer surface temperatures of high-arctic tundra on Svalbard – Implications for MODIS LST based permafrost monitoring. *Remote Sensing of Environment* **115**: 908-922.

Williams MW, Knauf M, Caine N, Liu F, Verplanck PL. 2006. Geochemistry and source waters of rock glacier outflow, Colorado Front Range. *Permafrost and Periglacial Processes* **17 (1)**; 13-33. DOI: 10.1002/ppp.535.

Wolf-Gladrow DA, Zeebe RE, Klaas C, Körtzinger A, Dickson AG. 2007. Total alkalinity: The explicit conservative expression and its application to biogeochemical processes. *Marine Chemistry* **106**: 287–300.

Zarnetske JP, Gooseff MN, Brosten TR, Bradford JH, McNamara JP, Bowden WB. 2007. Transient storage as a function of geomorphology, discharge, and permafrost active layer conditions in Arctic tundra streams, *Water Resour. Res*. **43**: W07410. DOI:10.1029/2005WR004816.

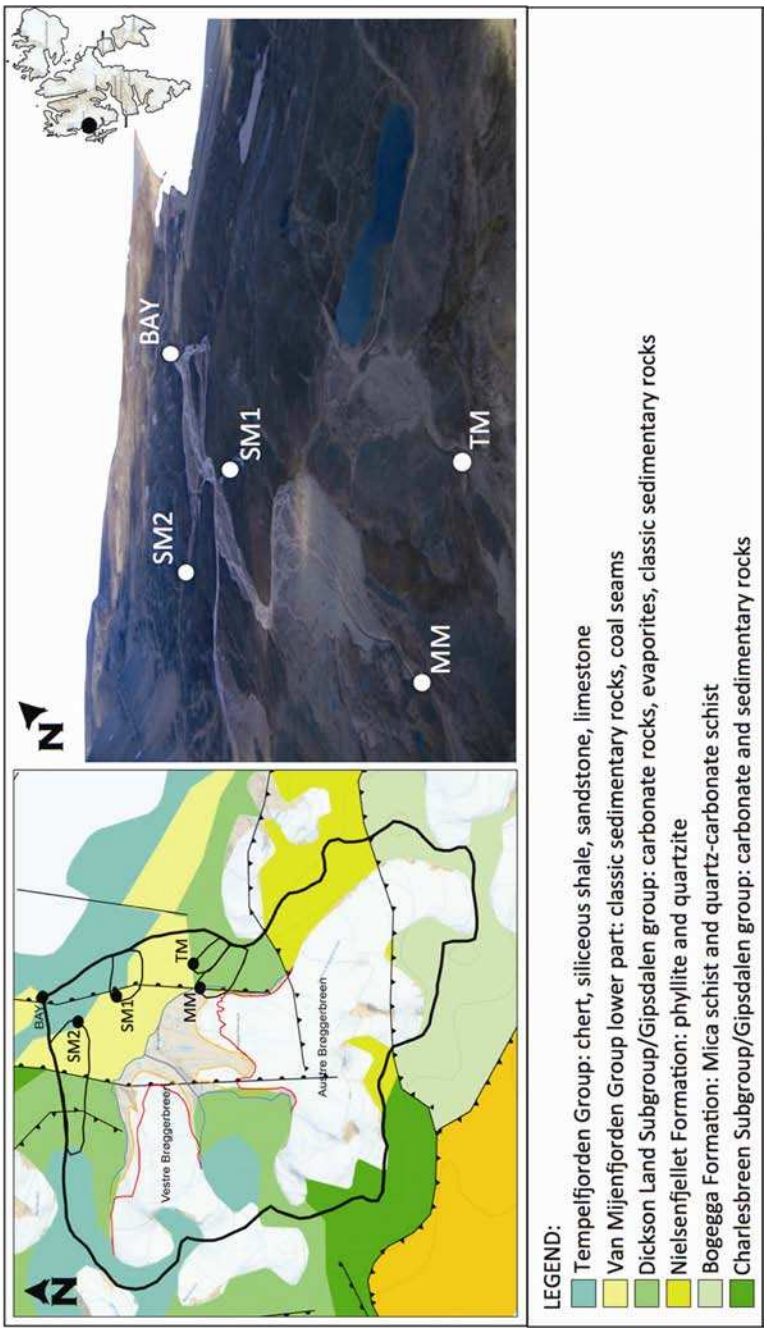

Fig. 1 The location of sampling sites in the Bayelva catchment on the Brøggerhalvøya, Svalbard and the geology of the watershed. Black lines indicate the borders of the micro-catchments (SM1, SM2, TM, MM) with their sampling points (dots) and the whole Bayelva watershed (BAY). The map was modified from Norwegian Polar Institute: www.svalbardkartet.npolar.no, 2013. Photo credit: A. Hodson

Fig. 2 Abandoned meltwater channel at MM (upper) and sampling location at MM Photo credit: A. Nowak

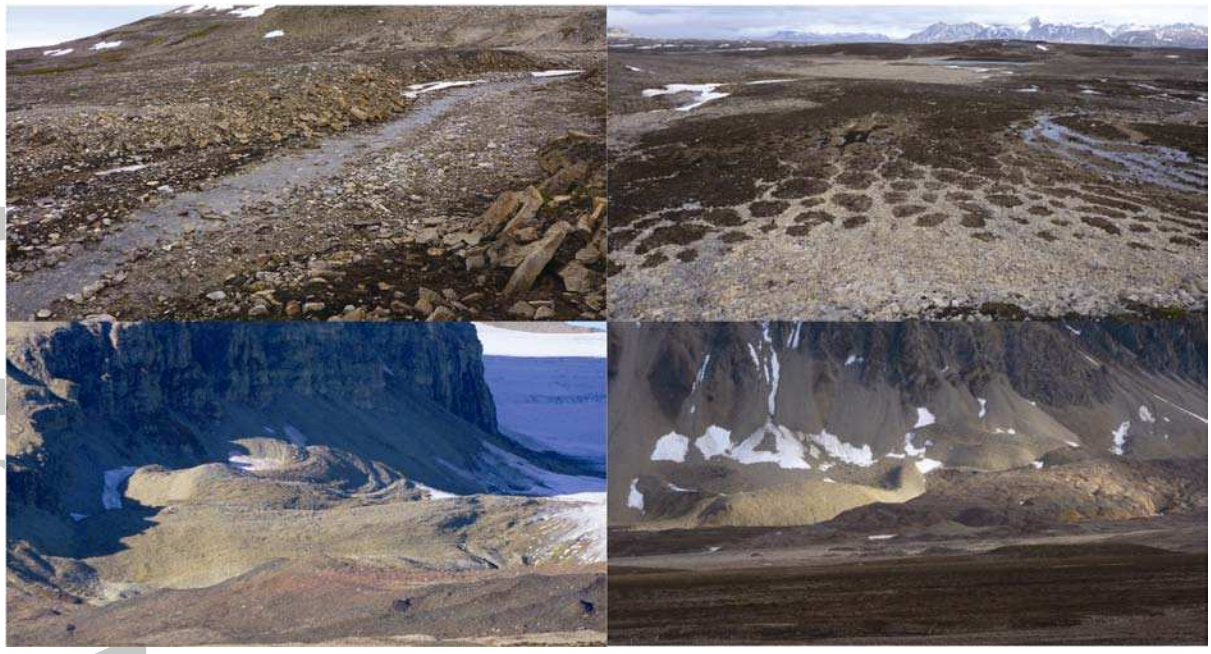

Fig. 3 Sampling location at TM (upper left), patterned ground in the northern part of the micro-catchment (upper right) and rock glacier in the southern part (lower left and right). Photo credit: A. Nowak

Fig. 4 Sampling location at SM1 (upper left and right) and SM2 (lower left and right). Photo credit: A. Nowak

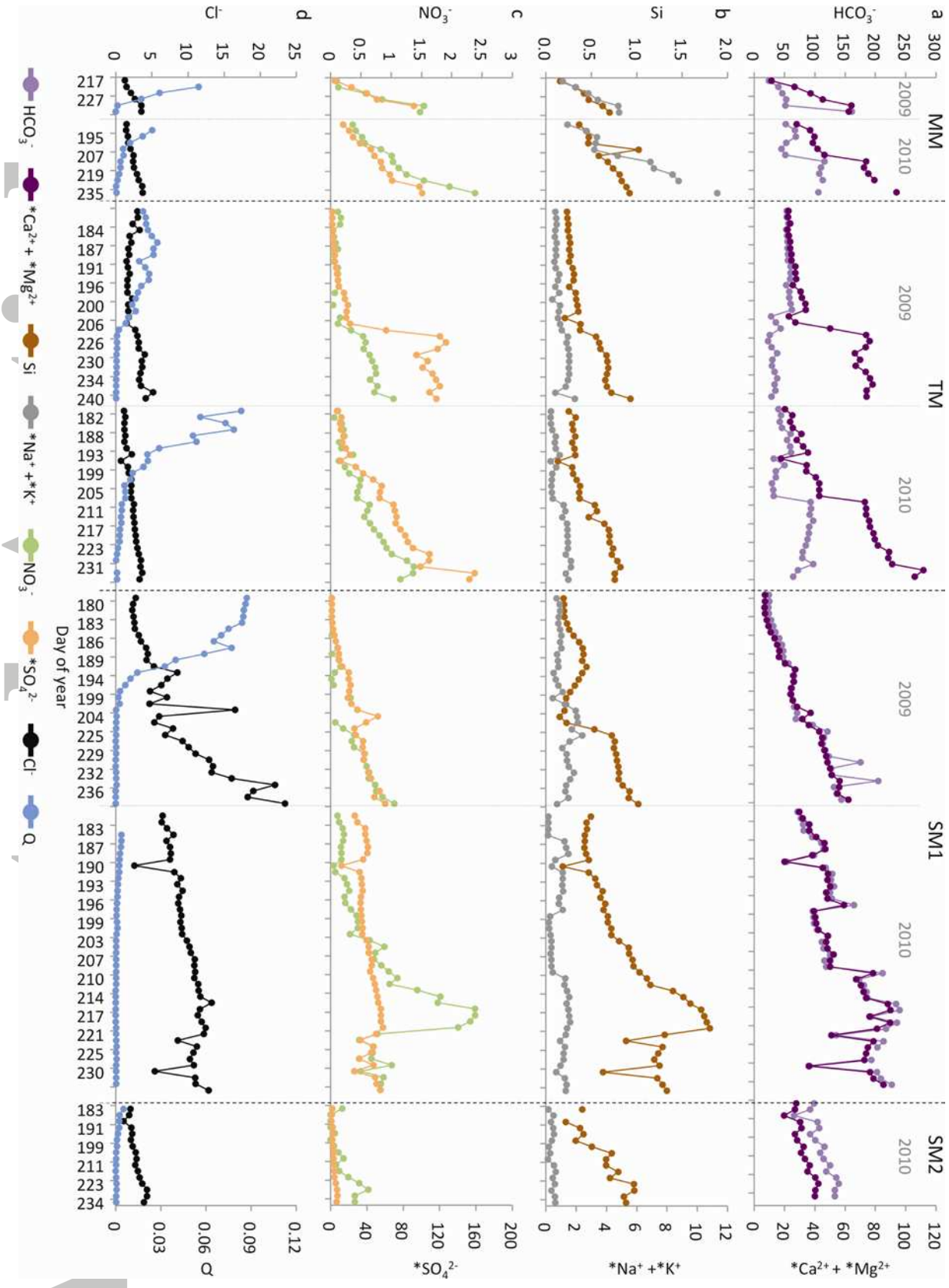

Fig. 5 Time series of ion concentrations (mg L^{-1}) and water discharge (m^3 sec^{-1}) at various sampling sites in the Bayelva watershed during 2009 and 2010 ablation seasons.

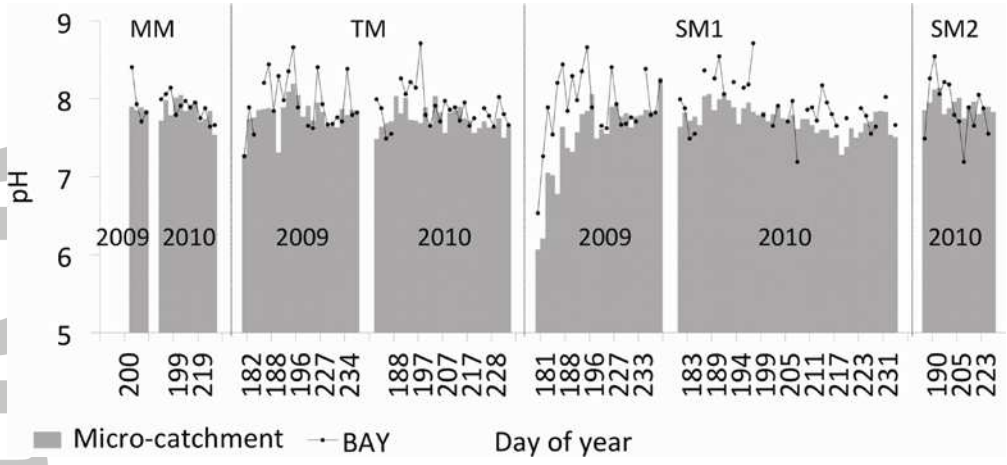

Fig. 6 The change in stream pH at all micro-catchments and in the Bayelva during 2009 and 2010 ablation seasons. Bayelva data are taken from Nowak and Hodson (In Press)

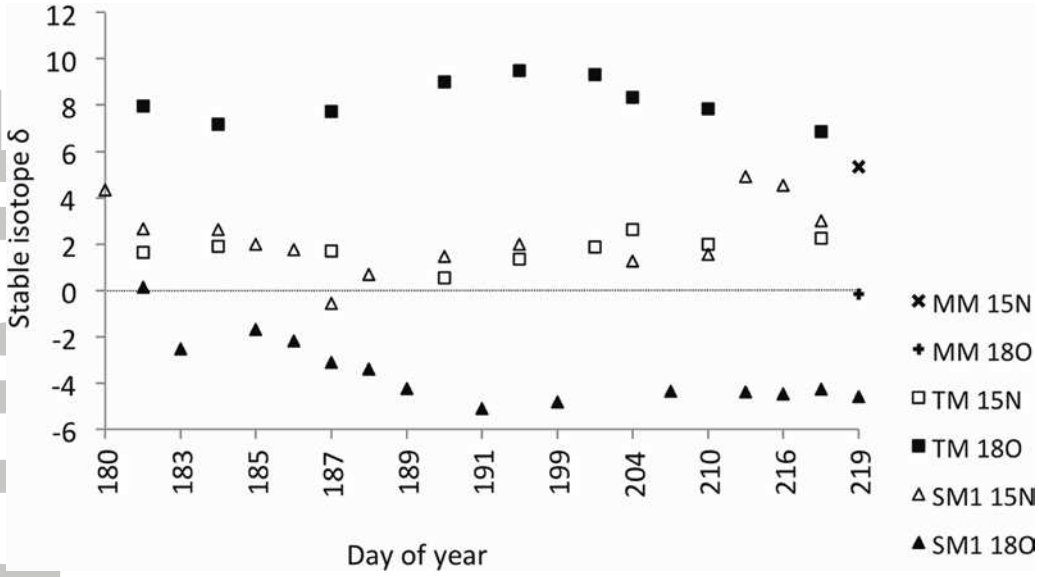

Fig. 7 Timeseries of stable isotopes $\delta^{15}N\text{-}NO_3^-$ and $\delta^{18}O\text{-}NO_3^-$ recorded at MM, TM, SM1 micro-catchments in 2010

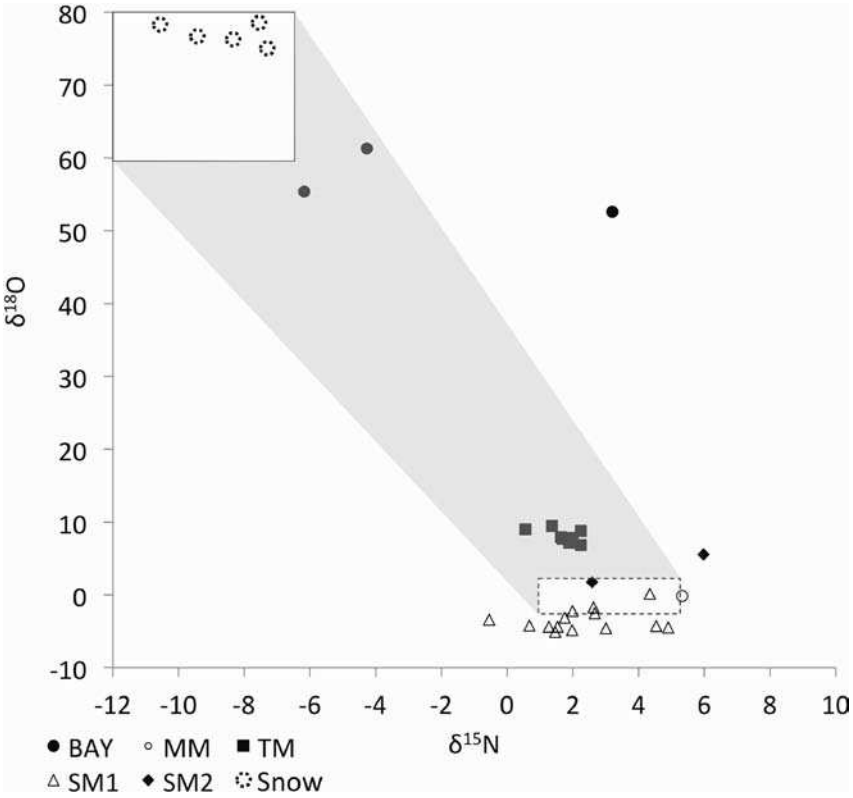

Fig. 8 Stable isotope results for δ^{15}N-NO_3^- and δ^{18}O-NO_3^- in the Bayelva and the micro-catchments during 2010. The solid box represents the range of values for snow in the general study area as reviewed whilst the open circles represent snowpack samples from 2010 (after Ansari et al., 2013). The hatched rectangle is the range of "microbial NO_3^-" values estimated by assuming the nitrification of soil organic N or snowpack NH_4^+ with minimal fractionation (Equation 1 in Ansari et al., 2013) and input ranges of δ^{18}O-H_2O (-15 to -6.8 ‰) and δ^{15}N -NO_3^- (1.2 to + 5.2 ‰) derived for local soils (Tye and Heaton 2007), ground ice (Budantseva et al., 2010) and non-ornithogenic, marine-derived soils (see discussion in Yuan et al., 2009). The grey shaded area is the hypothetical zone for mixed NO_3^- derived from the atmospheric and microbial sources

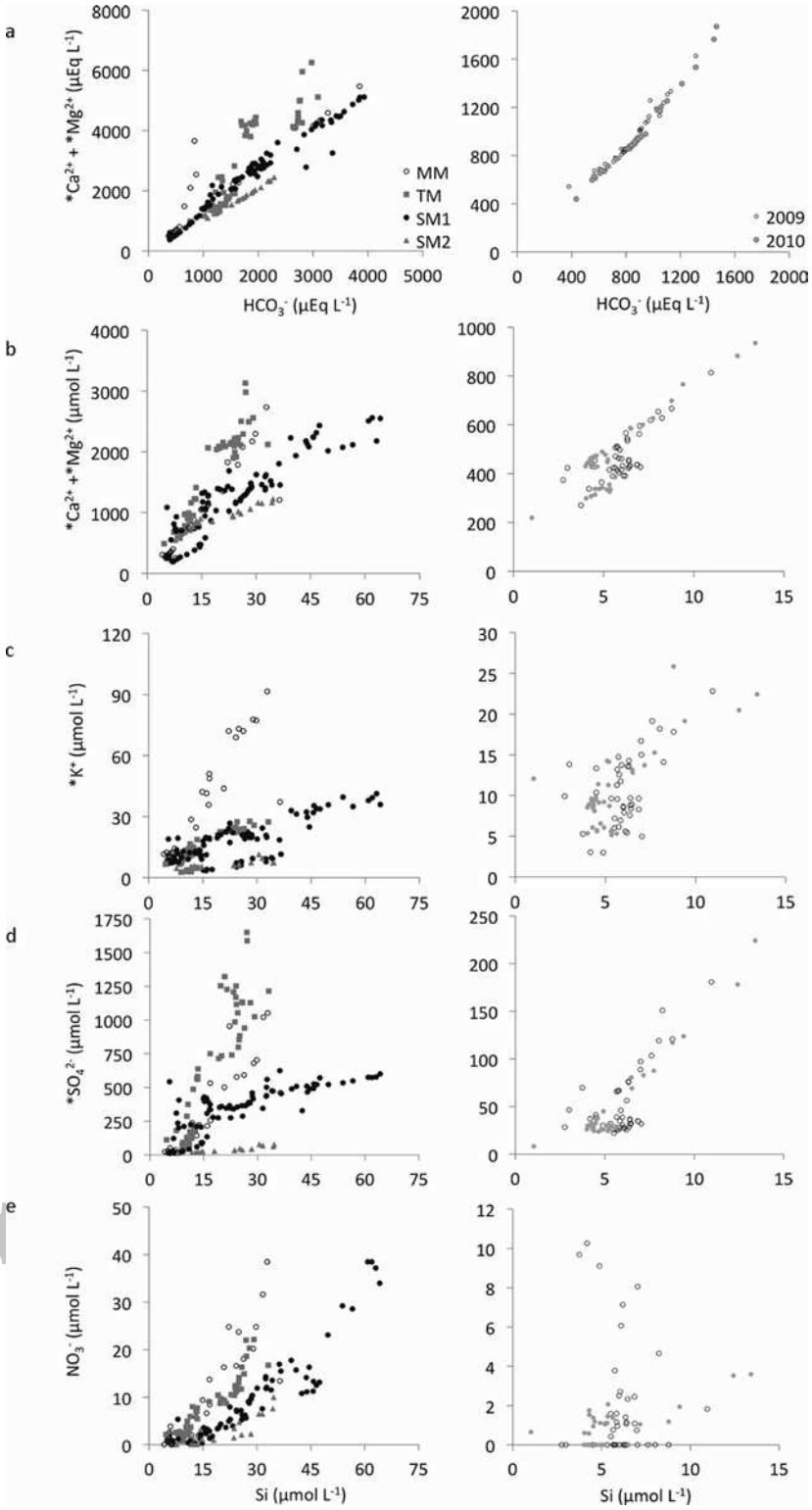

Fig. 9 The comparison of relationships between ions recorded at MM, TM, SM1, SM2 (left hand side) to those recorded at BAY (right hand side) during the 2009 and 2010 ablation seasons

Fig. 10 Bivalves in the uplifted marine sediments at SM1. Photo credit: A. Nowak

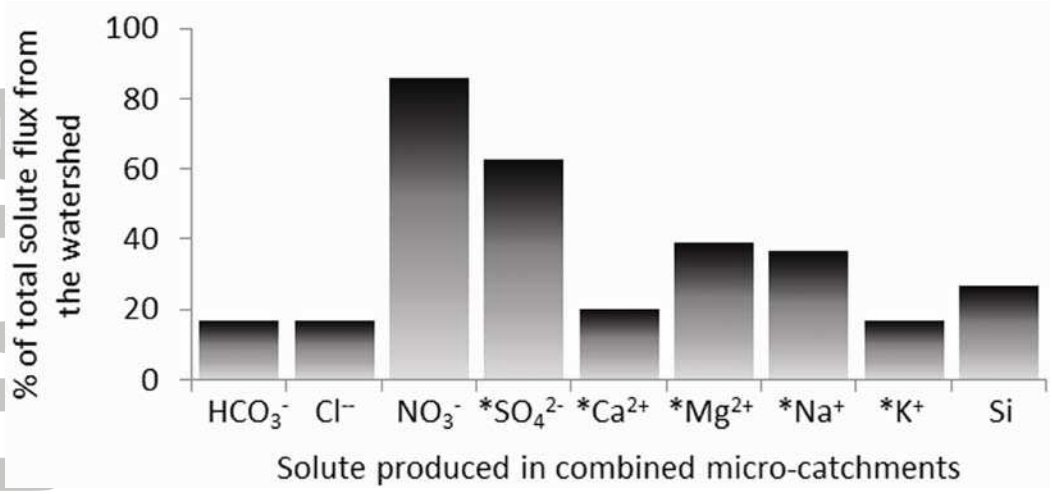

Fig. 11 Solute flux from combined micro-catchments expressed as a proportion of the total watershed solute flux measured at the BAY in 2010

Table 1 Comparison of sampling sites in Bayelva watershed including locations, areas and a basic description of their hydrology. [1]Discharge calculated for the 13 days period

Micro-catchment	Location	Area (km^2)	Specific discharge (m)		Water regime
			2009	2010	
Moraine (MM)	78°54.807N 11°50.647E	0.33	0.01[1]	0.16	Snowmelt, rainfall, ground ice melt including buried glacier ice
Talus (TM)	78°54.808N 11°51.630E	0.39	0.11	0.22	Snowmelt, rainfall, ground ice melt including rock glacier ice
Soil (SM1)	78°55.460N 11°49.903E	0.25	0.47	0.02	Snowmelt, rainfall, ground ice melt
Soil (SM2)	78°55.706N 11°48.040E	0.67	n/a	0.01	

Table 2 The comparison of sampling strategies and hydrological monitoring within the pro-glacial area of the Bayelva watershed in Svalbard during 2009 and 2010 melt seasons. [1] -sampling after the snowmelt phase; [2] - data logger was moved to another location when the main water flowpath from Austre Brøggerbreen changed due to glacier retreat

Site	Year	Sampling period		Sampling	Bayelva discharge period		Data logger	Manual stream flow measurement
		Dates	Days		Dates	Days		
MM	2009	13 June – 9 September	89	Daily, [1]every 2nd day	8 June – 26 September	111	CR 800, [2] n/a	Every 2nd day
TM				Daily, [1]every 2nd day			n/a	Every 2nd day
SM1				Daily			CR 800	Daily
MM	2010	29 June – 23 August	56	Every 4th day	18 June – 9 September	84	n/a	Every 4th day
TM				Daily, [1]every 2nd day			CR 800	Every 2nd day
SM1				Daily			CR 1000	Daily
SM2				Every 3rd day			n/a	Every 3rd day

Table 3 The comparison of ion yields from the micro-catchments and the whole Bayelva watershed during 2009 and 2010 ablation seasons. [1]Yields were calculated for 13 day period

Site	Year	HCO_3^-	Si	Cl^-	NO_3^-	$*SO_4^{2-}$	$*Ca^{2+}$	$*Mg^{2+}$	$*K^+$	$*Na^+$
		(kg km^2a^{-1})								
[1]MM	2009	922	3	19	7	443	264	71	15	24
TM		8023	46	306	21	2211	3495	833	67	48
SM1		18548	139	1667	19	2624	4412	1275	187	229
BAY		50931	149	2556	73	4321	13867	2387	404	210
MM	2010	24476	67	286	103	3665	4492	1566	250	266
TM		13107	82	374	58	5013	6430	1644	75	60
SM1		2444	13	183	7	831	750	241	11	3
SM2		1163	5	24	2	27	241	90	4	3
BAY		31981	91.1	686	26	2285	9108	1309	239	105

Table 4 The regression models between the aqueous products of well-known weathering processes recorded at various micro-catchments in the Bayelva watershed during 2009 and 2010 ablation seasons. R^2 values indicate the likelihood of the occurrence of the weathering process while slopes and intercepts indicate respectively stoichiometry of different weathering reactions and whether alternative mechanism(s) of chemical weathering supply any given solute.

Site	Regression Model No.	1	2	3	4	5	6	7	8	9
	X	HCO_3^-	$*Mg^{2+}$	$*Mg^{2+}$	HCO_3^-	$*SO_4^{2-}$	$*SO_4^{2-}$	Si	Si	Si
	vs	vs	Vs	vs	vs	vs	vs	vs	vs	vs
	Y	$*Ca^{2+}+*Mg^{2+}$	$*Ca^{2+}$	$*SO_4^{2-}$	$*SO_4^{2-}$	$*Ca^{2+}$	NO_3^-	NO_3^-	$*K^+$	$*SO_4^{2-}$
		($\mu Eq\ L^{-1}$)						($\mu mol\ L^{-1}$)		
SM1	R^2	0.96	0.97	0.90	0.73	0.80	0.54	086	0.62	0.60
	Slope	1.28±0.03	2.07±0.04	1.16±0.05	0.30±0.02	2.32±0.13	0.03±0.003	0.59±0.03	0.52±0.05	8.27±0.79
	Intercept	144±64.6	-81.6±41.3	48.9±35.7	141±44.9	83.1±103	-9.70±2.40	-7.22±0.97	4.97±1.40	135±23.8
SM2	R^2	1.00	0.36	0.54	0.83	0.83	0.85	0.75	0.57	0.85
	Slope	1.13±0.02	0.93±0.33	2.66±0.66	0.12±0.02	5.11±0.63	0.07±0.01	0.31±0.05	0.16±0.04	2.29±0.26
	Intercept	-161±32.7	586±229	474±57.8	-148±27.8	827±55.0	-1.98±0.64	-3.63±1.12	3.30±1.03	-11.7±6.01
TM early season	R^2	0.76	0.88	0.93	0.38	0.78	0.78	0.44	0.29	0.62
	Slope	1.73±0.16	2.23±0.14	0.48±0.02	0.74±0.16	1.04±0.09	0.01±0.001	0.64±0.12	0.94±0.25	60.0±7.99
	Intercept	-596±232	114±78.8	316±13.2	-593±229	828±55.3	0.85±0.30	-3.87±1.39	-0.51±2.85	-451±90.9
TM late season	R^2	0.09	0.37	0.23	0.05	0.81	0.01	0.92	0.46	0.04
	Slope	0.61±0.66	2.04±0.88	0.12±0.08	-0.45±0.65	0.76±0.12	-0.001±0.004	0.62±0.06	0.38±0.14	-5.51±9.14
	Intercept	3047±1205	199±1146	1017±176	3180±1200	1059±291	14.3±9.00	-3.57±1.52	14.6±3.33	1308±222
MM early	R^2	1.00	0.98	0.97	0.92	0.91	0.95	0.81	0.69	0.85

season	**Slope**	1.41±0.01	1.71±0.05	1.01±0.04	0.48±0.03	1.70±0.11	0.01±0.001	0.58±0.06	1.76±0.25	20.4±1.85
	Intercept	-16.4±13.1	251±26.2	92.1±16.7	-162±33.2	416±47.6	0.64±0.29	-1.89±0.78	1.78±3.24	-88.5±23.7
MM late	**R^2**	0.78	0.99	0.99	0.67	0.98	0.97	0.90	0.98	0.95
season	**Slope**	5.23±1.61	1.82±0.10	0.56±0.03	2.90±1.19	1.09±0.10	0.014±0.001	1.38±0.23	3.45±0.22	54.4±7.19
	Intercept	-1594±1163	343±81.5	111±27.0	-1160±859	520±104	-1.76±1.58	-9.52±3.92	-8.91±3.87	-336±110

Model 1. Establishes stoichiometry of carbonate weathering. For example, slope close to 1 indicates carbonation, while close to 2 indicates dissolution. However, additional sources of ions (in this case $*Ca^{2+}$ + $*Mg^{2+}$) can sometimes significantly increase the slope. Furthermore, an uptake of ions (for example creation of secondary mineral like gypsum) can decrease the slope. The judgment on which reaction is taking place depends on comparison to other regression models, catchment geology and chemical weathering kinetics. Significant, positive intercepts indicate that other processes are responsible for acquisition of ion(s) placed on *Y* axis, in this case $*Ca^{2+}$ + $*Mg^{2+}$ such as silicate weathering or gypsum/anhydrite dissolution, while significant negative intercepts indicate an additional source of ion(s) on *X* axis, in this case HCO_3^-

Model 2. Establishes relative importance of dolomite as a carbonate source of $*Mg^{2+}$

Model 3. Establishes importance of sulphide oxidation as a driver of the $*Mg^{2+}$sources presented above

Model 4 *and* ***Model 5*****.** Establishes importance of sulphide oxidation coupled to carbonate dissolution, resulting in a slope close to 1. Large intercept identifies other processes influencing $*SO_4^{2-}$ concentrations such as gypsum/anhydrite dissolution

Model 6**.** Establishes relationship between NO_3^- production and $*SO_4^{2-}$ production, which are both largely assumed to be microbially-mediated

Model 7. Establishes relationship between NO_3^- production and longer residence time flowpaths conducive to silicate weathering, or uptake of both solutes during diatom blooms

Model 8. Establish stoichiometries of silicate weathering and/or relative importance of K-feldspars

Model 9. Establishes importance of sulphide oxidation as a driver of silicate weathering